Polymer 50 (2009) 3747–3754

Contents lists available at ScienceDirect

Polymer

journal homepage: www.elsevier.com/locate/polymer

Effect of melting and crystallization on the conductive network in conductive polymer composites

Hua Deng [a], Tetyana Skipa [c], Rui Zhang [a], Dirk Lellinger [c], Emiliano Bilotti [a], Ingo Alig [c], Ton Peijs [a,b,*]

[a] Queen Mary University of London, Centre of Materials Research, School of Engineering and Materials Science, Mile End Road, E1 4NS London, UK
[b] Eindhoven University of Technology, Eindhoven Polymer Laboratories, 5600MB Eindhoven, The Netherlands
[c] Deutsches Kunststoff-Institut (DKI), Schlossgartenstrasse 6, D-64289 Darmstadt, Germany

ARTICLE INFO

Article history:
Received 18 August 2008
Received in revised form
4 March 2009
Accepted 10 May 2009
Available online 20 May 2009

Keywords:
Nanocomposites
Carbon nanotubes
Conductive network

ABSTRACT

Investigation on the effect of melting and crystallization of polypropylene (PP) on the conductive network of multi-wall carbon nanotubes (MWNTs) and carbon black (CB) in MWNT/PP and CB/PP composites is performed. The conductive networks formed by fillers with different aspect ratios (MWNTs and CB) are compared during melting and cooling experiments. The network is found to be deformed during melting and re-constructed again due to the re-agglomeration of fillers during isothermal annealing of the melt. Both deformation and re-construction of the network result in a substantial increase/decrease of the thermal resistivity of MWNT/PP and CB/PP composites. For the modelling of the dynamic network reformation three different approaches are tested: classic percolation theory, general effective medium theory (GEM) and Fournier equation.

1. Introduction

Polymer composites reinforced with carbon nanotubes (CNTs) have been investigated extensively since the last decade. Bulk composites reinforced with CNTs have been investigated regarding mechanical, thermal, electrical and other properties as reviewed in [1–4]. The processing methods utilized are mainly solution based, in situ polymerization and melt compounding. The mechanical reinforcement potential of CNTs in bulk polymer composites is high, but the theoretical strength of CNTs is only approached if a high level of dispersion, interfacial interaction and alignment of nanotubes is achieved in oriented systems such as polymer fibres and tapes [3,5].

Lately, the activity in exploiting exceptional properties of CNTs in polymer composites has focused on conductive polymer composites (CPCs). CPCs are conventionally made by adding carbon black, metal powder or carbon fibre into a polymer matrix [6,7]. Even with the polymer (or ceramic [8]) matrix being an insulator; the conductivity of the composites can demonstrate a sudden jump when a critical filler content is reached. This phenomenon is often described as percolation [9,10]. The percolation threshold of composites has been shown both experimentally and theoretically to decrease with increasing the filler aspect ratio [11–13]. CNTs have become one of the most interesting fillers for CPCs, since their large aspect ratio and excellent conductivity [4] can result in exceptional low percolation thresholds [14–16].

In order to process CPCs into desired shape, composites have to undergo processing steps such as: injection moulding, spinning or stretching. During these processes the conducting networks are deformed to different extents. Some studies have been carried out in order to investigate the influence of processing conditions on the conducting network [17–20]. It is shown that conductive networks can be reformed in the melt for CPCs filled with both MWNTs [17,18,21–26] and CB [27–30].

Real-time tracing of the dependence of electrical resistivity during isothermal heat treatment on isotropic CPC containing CB is carried out by Wu et al. [27]. In this research, an interesting delay of percolation time in CPC is found: a percolation time is needed for the composites to be annealed above their glass transition temperature in order to form a conductive network. They concluded that percolation is delayed by the bulk mobility of the polymer layer around CB particles. Therefore, the formation of a conductive network by conductive fillers in a polymer matrix is greatly influenced by thermodynamic interactions between filler and matrix [30,31]. Thus, the polymer matrix viscosity, moulding temperature and time during processing plays an important role on the final resistivity. Research in this area on MWNT/polymer composites [17,18,21,22] has shown similar effects. A model based on re-aggregation of MWNTs in the melt is proposed to explain the re-construction of the conductive network in a polymer melt. It was

* Corresponding author at: Queen Mary University of London, Centre of Materials Research, School of Engineering and Materials Science, Mile End Road, E1 4NS London, UK. Tel.: +44 (0)207 882 8865; fax: +44 (0)208 981 9804.
E-mail address: t.peijs@qmul.ac.uk (T. Peijs).

0032-3861/$ – see front matter © 2009 Elsevier Ltd. All rights reserved.
doi:10.1016/j.polymer.2009.05.016

found that a high MWNT content in the matrix results in a strong network, thus, a thermal treatment has less effect on resistivity changes in these CPCs compared to CPCs containing less nanotubes. Previously, similar re-aggregation of MWNTs in a polymer matrix has been reported by our group [32]. Another issue Alig et al. pointed out in their studies is the thermo-mechanical history of the CPC which plays a significant role on the final resistivity of the specimen. Therefore, in the present study the thermo-mechanical history for all investigated CPCs was identical.

Non-isothermal annealing of CPCs containing CB was studied by Zhang et al. [28]. A positive temperature coefficient (PTC) and negative temperature coefficient (NTC) in resistivity of composites during melting is observed. The PTC effect is explained by the melting of the crystalline phase of the matrix. The transformation of crystalline into amorphous phase is associated with a significant volume expansion of the matrix. It results in an increased inter-particle distance of the conductive fillers and reduces the probability for the electrons to tunnel between the particles in the expanded conductive network. In contrary the NTC effect is thought to be due to the re-aggregation of conductive fillers in a polymer melt as explained above.

The effect of crystallization of a polymer matrix on the electrical conductivity of MWNT/polypropylene composites was investigated by Alig et al. [17]. They reported that DC conductivity of the CPC decreases by more than one order of magnitude during crystallization. It is explained by the reduction of the amount of amorphous phase in which ion conductivity is the dominating mechanism.

It is the purpose of this study to investigate the effect of melting, thermal annealing and crystallization on the conductive network in isotropic CPCs. MWNTs and CB are used as conductive fillers while inline electrical measurement is used to monitor the state of the conductive network during thermal annealing. Three different percolation models coupled to the cluster agglomeration approach are used to fit and explain the experimental results.

2. Experimental

2.1. Materials and composite preparation

MWNTs (Nanocyl® 7000) used in this study were kindly provided by Nanocyl S.A. (Belgium). The MWNTs were produced by catalytic carbon vapor deposition (CCVD) process with diameter approximately 10 nm and length of 1.5 μm, its surface area is in the range of 250–300 m^2/g according to the supplier [33]. The conductive carbon black (CB) used is Printex® XE-2 which is a highly structured CB supplied by Grolman Ltd. A study by Pantea et al. [34] of several CBs demonstrated that CPCs based on Printex® XE-2 showed a high level of conductivity compared to other CBs due to their high surface area (910 m^2/g). The polypropylene used in this study is a random ethylene–polyprolene co-polymer with 2% ethylene and 98% propylene. It is produced by Basell (Adsyl 5C39F: $M_w = 320$ kg/mol, MFI = 5.5 g/min, polydispersity is 4.3). MWNTs or CB are melt compounded with PP in a micro-extruder (DSM Explore Micro 15) at 200 °C, 200 rpm for 10 min. The extruded strand is then cut and hot pressed into sheets of 150 μm thick at 200 °C for 5 min. Samples of 5 mm × 20 mm are then cut from these sheets and then placed in an oven for inline electrical measurements. The experimental setup is schematically shown in Fig. 1.

2.2. Composite characterization

TEM

The morphology of primary CB and MWNTs aggregates is examined by transmission electron microscopy (TEM) using a JEOL JEM-2010 TEM in order to understand their internal structure before their incorporation into the polymer matrix. Specimens were prepared by dispersing CB and MWNT powders in ethanol using ultra-sonication. The specimens were picked up by a copper grid, and left for solvent to evaporate. The aggregates of CB and MWNTs that remained on the copper grid were studied in TEM. The mean size of the CB particles was estimated to be of 50 nm, while the primary agglomerate size extends to 600 nm (Fig. 2a). MWNTs are mostly separated from primary bundles and have diameters of about 10 nm (Fig. 2b).

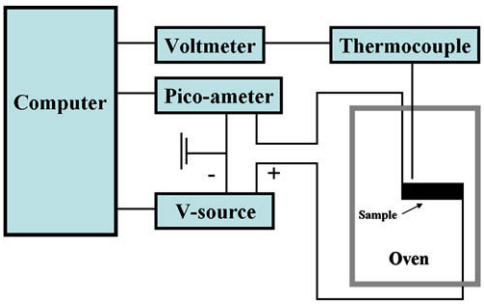

Fig. 1. Sketch of experimental setup for inline measurement of the effect of annealing on electrical resistivity of CPC.

SEM

Scanning electron microscopy (SEM) studies of the morphology of MWNT and CB conductive networks in CPC are carried out on a JEOL JSM-6300F SEM using high accelerating voltage. As demonstrated by

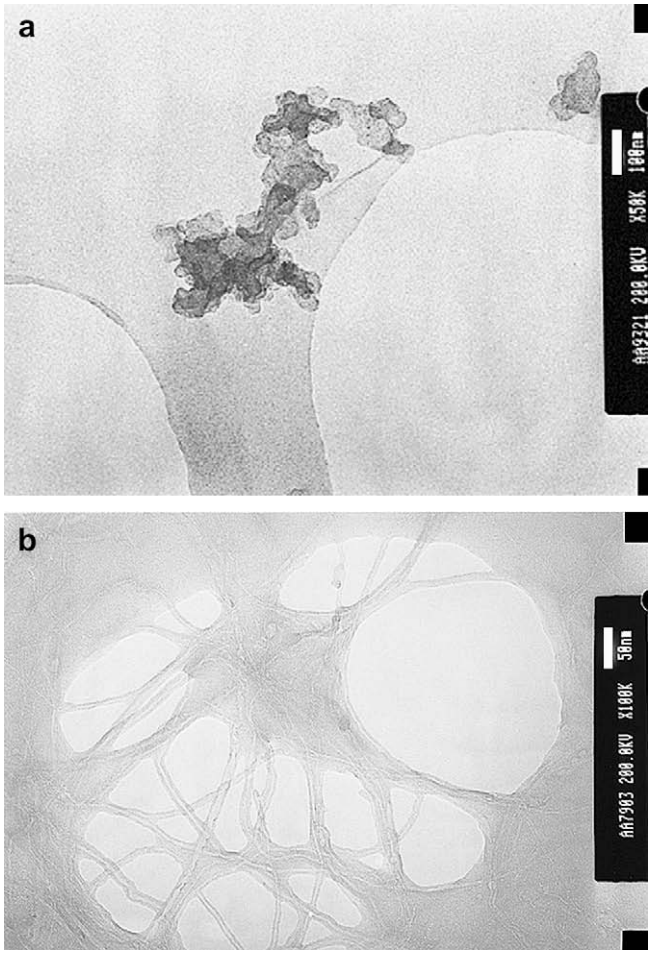

Fig. 2. TEM picture of the fillers used in this study, (a) CB and (b) MWNTs as received.

Loos et al. [35], MWNTs or CB in a polymer matrix material are charged to give an enriched secondary-electron current, making SEM a valuable tool for studying the nanofiller networks in CPCs. In Fig. 3a, the structure of the conductive network in CB/PP with 15 wt.% CB is shown. The spherical agglomerates of CB seem to cover the whole PP matrix creating a 3D conducting network. In Fig. 3b a large MWNT island of approximately 10 μm consisting of interconnected agglomerates of around 1 μm is presented for the CPC with 5.3 wt.% MWNT. It should be noted that both TEM and SEM studies show the 2D representative of a 3D conductive network where some of the underlying interconnected paths cannot be seen.

DSC

Differential Scanning Calorimetry (DSC) study is conducted in Mettler Toledo DSC 822^e at a heating rate of 10 °C/min from 20 °C to 200 °C for all the CB and MWNT concentrations. The crystallization and melting curves provide information on thermal behaviour of the composites as well the influence of nanotubes on the crystallization of PP matrix.

Inline electrical measurement

Automated inline direct current (DC) electrical measurement setup is shown in Fig. 1. Voltage scan is chosen to be 1 V to avoid a strong electrical current through the sample. In order to minimize a constant electrical field on the sample, 300 ms internal voltage (0 V) is applied for every 700 ms (1 V). Silver paint is applied on both ends of the sample to insure good contact. High temperature resistance polymer coated copper wire is used in the oven to connect the sample with electrodes and wires outside. The specimen is kept on a PTFE plate during the experiment to maintain its shape. The thermal couple reads the temperature of the air close to the surface of the sample as shown in Fig. 1.

Rheology

A rheological study is carried out in a TA Instruments Advanced Rheometer 2000 equipped with a TA Instruments environmental test chamber. The measurements were carried out in dynamic mode and 25 mm parallel plate geometry with a gap setting of 1 mm under liquid nitrogen atmosphere. A strain amplitude of 0.5% was chosen to be within the linear range. Frequency sweep was carried out between 0.02 and 625 rad/s.

3. Results and discussion

3.1. Morphology and thermal properties of the composites

The morphology of the CB and MWNT fillers and CB/PP and MWNT/PP composites is investigated with TEM and SEM,

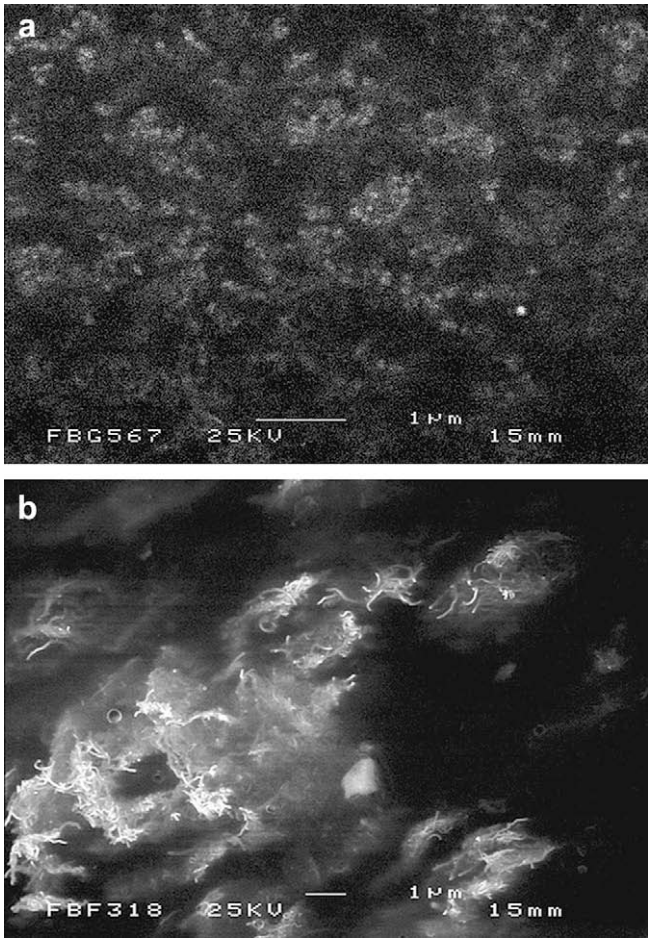

Fig. 3. SEM picture of the hot pressed composites, (a) 15 wt.% CB/PP and (b) 5.3 wt.% MWNT/PP.

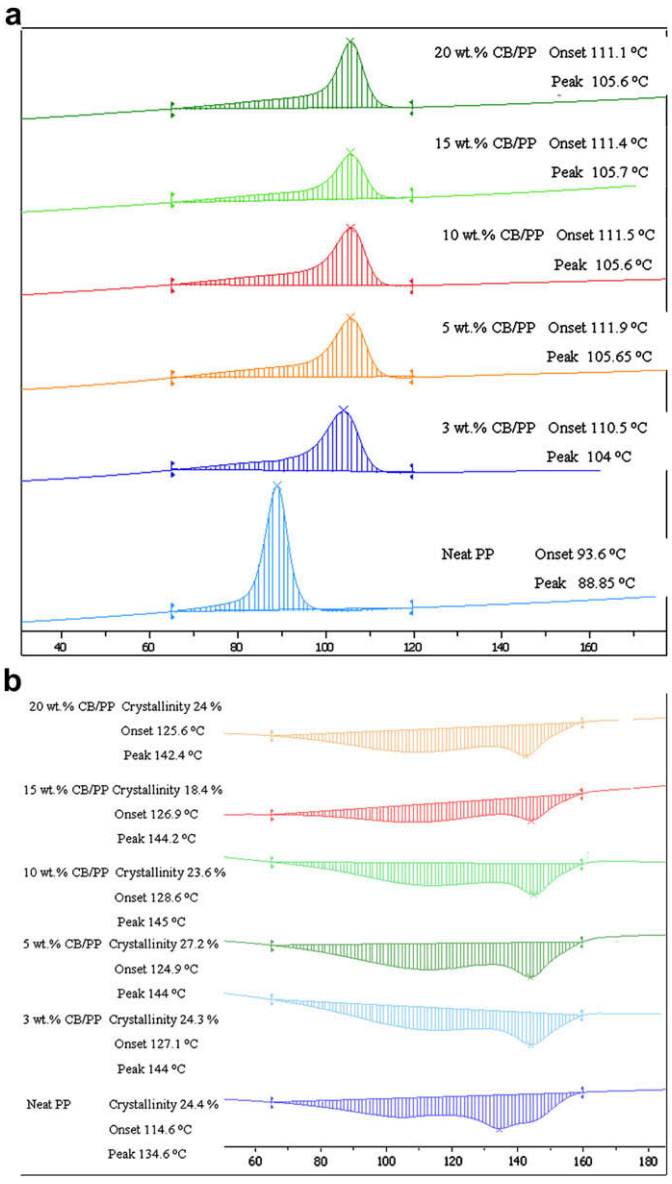

Fig. 4. DSC curves for CB/PP composites, (a) crystallization curves, (b) melting curves.

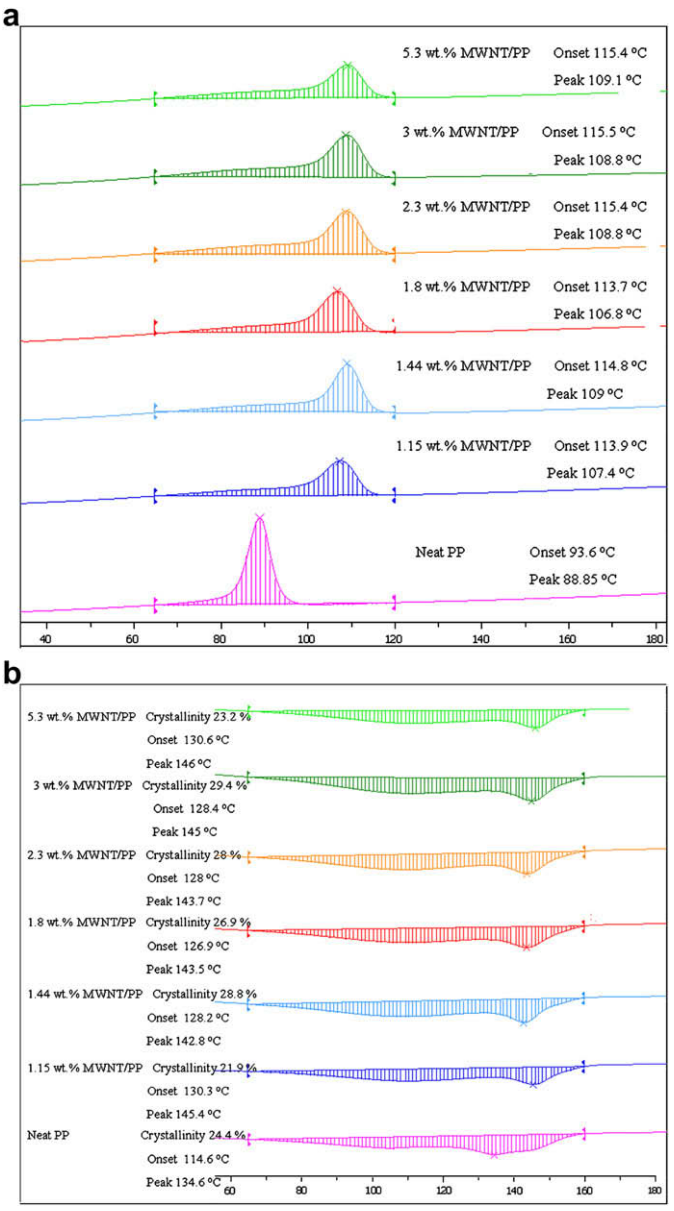

Fig. 5. DSC curves for MWNT/PP composites, (a)crystallization curves, (b)melting curves.

respectively, as shown in Figs. 2 and 3. Due to the large aspect ratio of nanotubes (see Fig. 2b), the networks formed by MWNTs are more likely to be entangled than the networks based on CB. As shown in Fig. 3, MWNTs are mainly dispersed as small bundles in the polymer matrix, while CB is dispersed in the form of primary aggregates. It was shown in a previous study that the conductive network formed by MWNTs is more stable under large deformations than the network formed by CB due to stronger physical entanglement between MWNTs as a result of their large aspect ratio [20]. It is expected that the deformation of the network during melting and crystallization should also reflect this high degree of the entanglement of filler particles constituting the conductive network.

The thermal properties of the composites characterized by DSC are shown in Figs. 4 and 5. The crystallinity of the PP used in this study is relative low (21–30%) compared with PP homopolymer, which is typically between 35–50% [36–38]. Both of the fillers are acting as nucleation agents for the PP polymer matrix during crystallization, resulting in an increase of the crystallization temperature for composites compared to the neat matrix (see Fig. 4a and Fig. 5a). However, further increase of the filler content has no obvious effect on the crystallization temperature of the composites. As the copolymer has a wide melting peak (see Fig. 4b and Fig. 5b), the melting temperature peak was shifted from 134.6 °C to near 145 °C indicating that both CB and MWNT fillers have changed the structure of polypropylene crystallites preventing them from melting at lower temperatures. The whole temperature range of melting peaks remains unchanged (from 80 °C to 160 °C) before and after adding different amounts of fillers to the matrix. For both CB/PP and MWNT/PP composites no significant change was detected in the crystallinity value compared to the neat polymer matrix. The melting temperatures of the CB/PP and MWNT/PP composites are similar for different filler content assuming a similar start of the melting process in a non-isothermal experiment. Isothermal annealing of the composites was done at 165 °C, well above their melting point.

3.2. *Electrical resistivity of the composites in melting/crystallization experiments*

Fig. 6 shows the temperature program for the oven in Fig. 1. The annealing time for the composites with different filler content in the following experiments are chosen according to the time needed to achieve a stabled individual resistivity. The annealing time at targeted temperature may vary for each specimen. The oven is switched off when a stable conductivity/resistivity value was obtained. Finally, the data recording is stopped after reaching room temperature for the specimen.

Inline electrical measurements are conducted during the whole thermal program on isotropic CPCs containing MWNTs or CB as shown in Figs. 7 and 8. The oven temperature is targeted at 165 °C until cooling begins (see Fig. 6). For each of the resistivity curves, except for the highest filler contents of CB and MWNTs, a peak was detected at a certain time during isothermal annealing. Similar effects of a decrease in resistivity are also known as positive temperature coefficient (PTC) while a resistivity increase is known as negative temperature coefficient (NTC) [28]. The increasing in resistivity is explained by dilution of the conductive filler network into the polymer melt from the amorphous phase in a semi-crystalline polymer. The conductive network is thus expanded in the melt which leads to a drastic decrease in the probability of the electron tunnelling between the parts of the expanded conductive

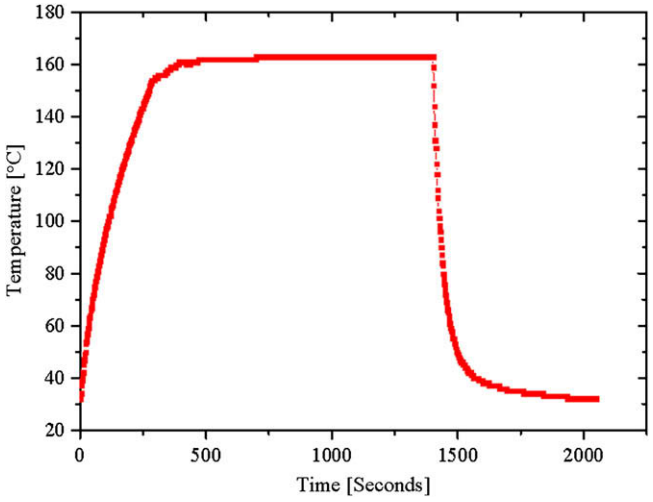

Fig. 6. Temperature profile of the oven in Fig. 1. Please note that isothermal annealing is performed until a stable current data is obtained, thus, the overall annealing time for each specimen might be slightly different.

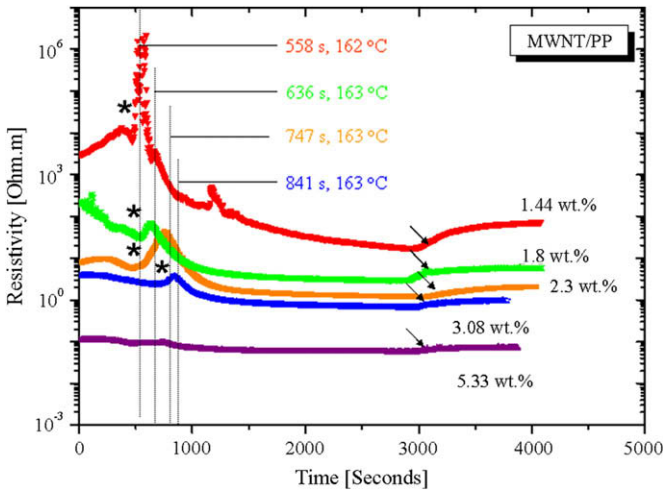

Fig. 7. Inline electrical measurement of isotropic MWNT/co-PP film at different MWNT content. The arrows indicate where the oven starts to cool down to room temperature.

network and could result in an increase of the composite resistivity. Such a jump in resistivity due to melting detected between 500 s and 850 s after starting the experiment is observed in Figs. 7 and 8 for both MWNT/PP and CB/PP composites, respectively. A prominent peak is observed for each curve except for the highest filler contents. The position of the peak along the time scale corresponds to the complete expansion of the network. The re-aggregation of MWNT or CB clusters was assumed to start here. Re-organisation of the conductive network in the melt has already been described in literature [18,27]. MWNT or CB clusters show strong ability to aggregate and build up connections between the broken network parts in the melt due to the complex interactions between them and with polymer matrix. It was also noticed for PP composites that the crystallization of the polymer matrix increases the overall resistivity due to freezing the conductive network in the amorphous phase and interruption of the contacts between conductive phases. However this effect is negligible for the resistivity of CPC containing large amounts of filler, because the conductive networks have been strongly built in the matrix.

An interesting conductivity behaviour (a local drop, marked with * in Fig. 7) of the MWNT/PP composites (absent for CB/PP composites) can be observed shortly before the complete melting of the polymer matrix. The following explanation could be preliminary proposed: at the beginning of the melting process small deformations and shifts in the polymer matrix could lead to densification of the nanotube network and the same deformation will break the connections in CB networks. This may indicate again that the entangled structure of MWNTs has a higher potential to maintain contacts during deformation (see inset in Fig. 9). Such a weak effect can be seen only for low MWNT concentrations when the fine percolative network is very sensitive to small morphological changes.

Another important difference in the position of the resistivity peaks for MWNT/PP and CB/PP can be noticed. With increasing MWNT content (Fig. 7) the resistivity peaks shift to longer times in contrast to the resistivity peaks for the CB/PP (Fig. 8) which do not show a distinct peak shift.

The peak shift observed in the case of MWNTs means that maintained contacts are longer during melting and expansion of the polymer matrix compared to CB networks.

In order to have a closer look at the difference between the conductive networks built up from MWNT and CB two resistivity curves were plotted together in Fig. 9: for the MWNT/PP composite with 2.3 wt.% MWNT and CB/PP with 5.0 wt.% CB. A schematic presentation of MWNT and CB clusters is given as an inset.

Both concentrations (2.3 wt.% MWNT and 5.0 wt.% CB) provide identical final values of the resistivity of the composites, although, the concentration ratio MWNT/CB is a factor of 0.5. The curves have the same kinetics of the network reformation what follows from their shape in the later time frames (after 742 s). This supports the idea of the cluster aggregation mechanism for network formation for both MWNT and CB fillers.

However, the most important difference is reflected in the resistivity peaks corresponding to ~573 s for MWNT/PP and ~743 s for CB/PP composites. Comparing the two resistivity plots, one can see that MWNTs are able to keep contacts in the network during annealing for about 170 s longer than the CB particles.

The local minimum (marked with *) in the resistivity of MWNT/PP which can be attributed to the MWNT network densification at the beginning of melting, does not appear for CB.

The interaction between MWNTs in the network is much stronger than between spherical CB, due to physical entanglement and the higher aspect ratio of the nanotubes. Consequently, CB clusters are more likely to break apart upon deformation. This geometrical advantage makes MWNTs more attractive conductive fillers to create conductive percolating networks that have to resist large deformations as often encountered during polymer processing [20].

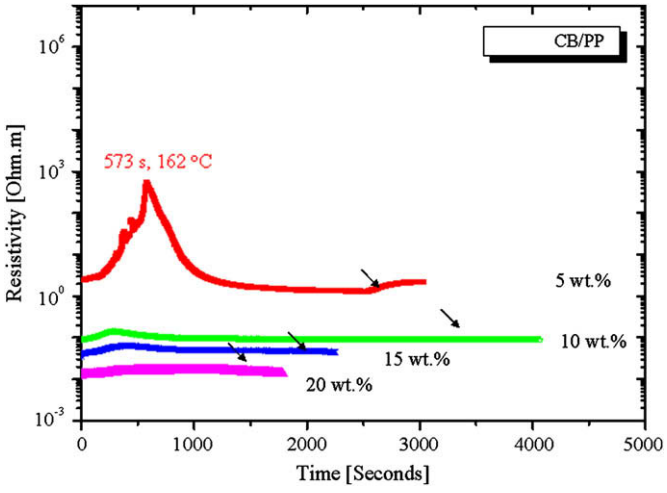

Fig. 8. Inline electrical measurement of isotropic CB/co-PP film at different CB content. The arrows indicate where the oven starts to cool down to room temperature.

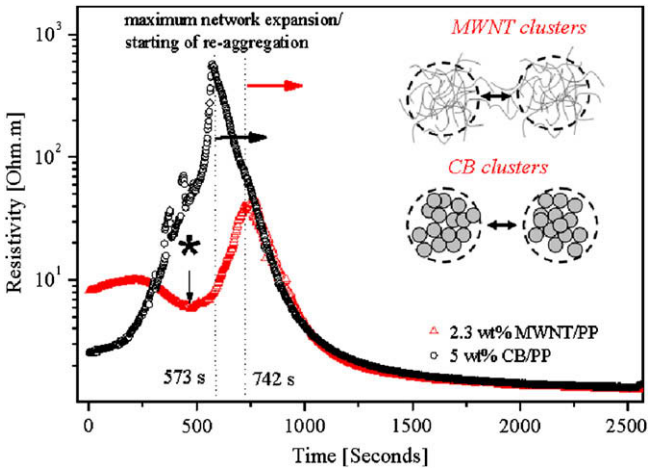

Fig. 9. Evolution of the resistivity curves for MWNT/PP with 2.3 wt.% MWNT and CB/PP with 5 wt.% CB with time during non-isothermal and isothermal experiment. Inset shows the schematic presentation of the MWNT and CB clusters.

All the specimens here underwent the same thermal history before melting and cooling, which is important since the thermal and electrical behaviour depends very much on the thermal history of the CPC. Based on that fact another interesting difference between MWNTs and CB composites should be discussed. By comparing the beginning and the end of the each curve in Figs. 7 and 8 (only CPCs containing small amounts of filler are considered here), the resistivity of the CPC filled with MWNTs is found to decrease after melting and crystallization while for CPC based on CB it remains nearly the same. The entangled and more stable network of MWNTs is believed to be responsible for this behaviour. Since all the composites have the same thermal history, the entangled networks formed by MWNTs are more resistant to thermal annealing during hot pressing (where re-aggregation occurs and local contacts between conductive clusters are repaired [26]) than networks formed by CB. Therefore, the melting and cooling process after hot pressing can lead to further perfection of the network.

3.3. Melt viscosity of the composites

To confirm that the effect described above is indeed caused by the morphological difference between MWNT and CB networks, the rheological properties of CPCs and neat polymer are investigated. The dynamic viscosity measured at 200 °C is plotted as a function of frequency in Fig. 10. The dynamic viscosity of CPCs based on CB and neat polymer are shown in Fig. 10a. The CPCs containing 20 wt.%, 15 wt.%, 10 wt.% and 5.0 wt.% CB reveal strong shear thinning effects, where the neat polymer shows only a small frequency dependence. Clearly the additional CB content in PP has increased the complex viscosity at all frequencies investigated. The effect of CB is most pronounced at low frequencies. This is in agreement with the established literature [39,40].

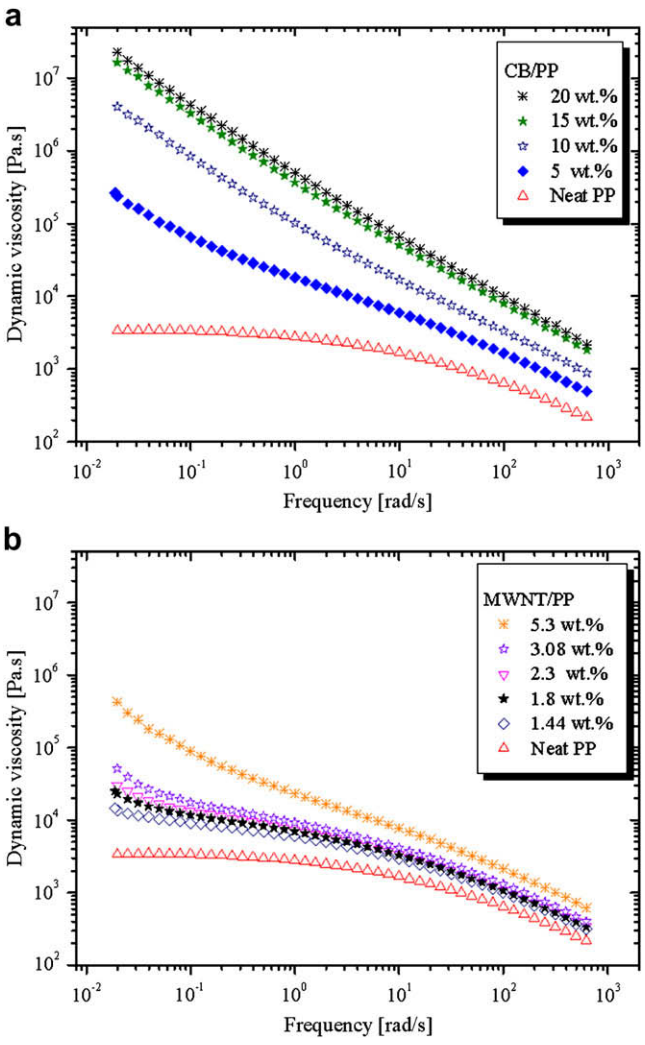

Fig. 10. Frequency dependence of dynamic viscosity of (a) CB/PP, (b)MWNT/PP.

Fig. 10b shows the dynamic viscosity of CPCs based on MWNTs and neat PP. The CPC containing 5.3 wt.% MWNT shows strong shear thinning effect, whereas the frequency dependence is much weaker for CPCs containing 3.08 wt.%, 2.30 wt.%, 1.80 wt.%, 1.44 wt.% MWNTs and neat PP. The additional MWNT content in PP has increased the complex viscosity at all frequencies investigated. However, the effect of MWNT is most pronounced at low frequencies. This is similar with the effect for CB shown in Fig. 10a.

By comparing Fig. 10a with b, there is little difference between 5.3 wt.% MWNT and 5.0 wt.% CB in the polymer matrix in terms of viscosity. However, there is indeed some difference in conductivity when composites containing the same amount of MWNT or CB filler are compared, as the higher aspect ratio of MWNTs results in higher conductivity. In the case of conductivity, properties are mainly determined by CNT–CNT networks in the system, whereas viscosity properties are determined by three different networks or interactions in the system [39]: CNT to CNT, polymer to CNT, and polymer to polymer. Therefore, in the case of a reduction in aspect ratio of the conductive filler (as in the case of replacing 5.3 wt.% MWNT with 5.0 wt.% CB), the conductive network is significantly affected, but the viscosity is not. In the current study, we compare two systems with similar viscosity (5.3 wt.% MWNT versus 5.0 wt.% CB) and the peak shift (as shown in Figs. 7–9) is still observed. When two systems with different viscosities (e.g. 2.3 wt.% MWNT and 5.0 wt.% CB, as shown in Fig. 9) are compared, the peak shift is also observed as indicated in the text. Therefore, the peak shift and the shape of the peaks (shown in Figs. 7–9) reported in this paper occur at different viscosities. They are caused by the fundamental difference between CB networks and MWNT networks, and they are not significantly influenced by viscosity of the system.

3.4. Modelling of conductivity recovery

As it was discussed above, melting of the polymer composite can lead to the destruction of the nanotube network and the conductivity drop (or appearance of the resistivity peak) due to the loss of

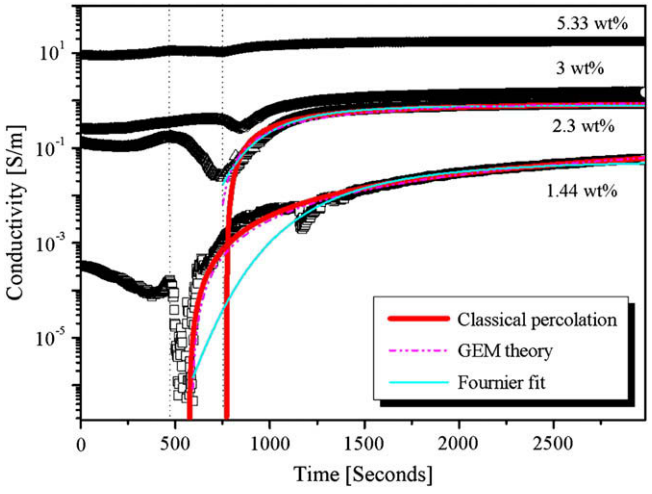

Fig. 11. Conductivity of CPCs containing MWNTs at different loadings and modelling of the conductivity recovery process using the: (1)cluster aggregation model combined with classical percolation theory, (2)Fournier equation and (3)GEM (see text for detail).

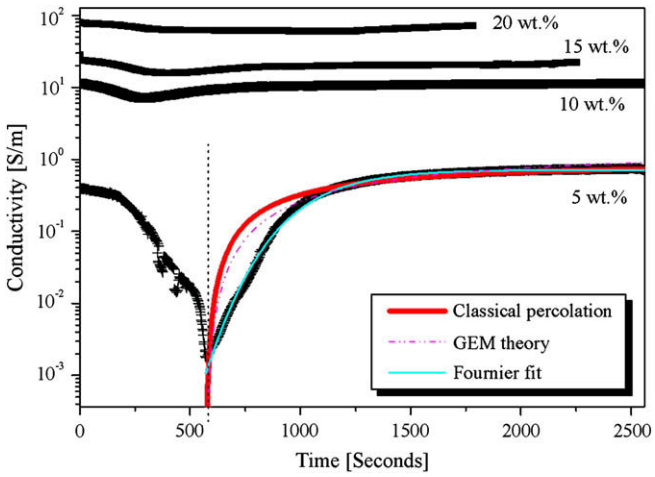

Fig. 12. Conductivity of CPCs containing CB at different loadings and modelling of the conductivity recovery: (1) cluster aggregation model combined with classical percolation theory, (2)Fournier equation and (3)GEM (see text for detail).

contacts between the network parts. During annealing, conductivity demonstrates a strong recovery effect with time (especially for low filler contents). This effect can be attributed to the reconstruction of the conductive network specific for polymer melts. In order to understand this process a simple picture was recently proposed by combining two approaches: (1) a model for aggregation of clusters and (2) the classical percolation theory for insulating/conductive systems [17,18].

The growth of the conductive network in polymer melts was considered as a process of agglomeration of the filler particles producing conductive sphere-like clusters. Those clusters (or agglomerates) occupy a much larger effective volume than fully dispersed nanotubes. At some volume concentration (close to that for percolation of spherical objects) the interconnected agglomerates create conductive pathways inside the polymer matrix leading to a drastic conductivity increase. This phenomenon is sometimes referred as dynamic percolation [22,29,41] and is more pronounced for low filler concentrations because of the large conductivity increase at the insulator–conductor transition [18,21,42].

For the modelling of the agglomeration process of nanotube clusters a second order kinetics was used [18,22,42]. This idea was first introduced by Heinrich et al. [42] for the formation of filler networks in elastomers. The solution of the kinetic equation gives a time dependent volume concentration of growing agglomerates:

$$p_A(t) - p_{A0} + (p_{A\infty} - p_{A0})\left(1 - \frac{1}{1 + 4kt(p_{A\infty} - p_{A0})}\right), \quad (1)$$

where p_{A0} and $p_{A\infty}$ are values of the starting and final (for $t \to \infty$) volume concentration of the agglomerates, respectively, and k is the reaction rate.

The classical theory of the electrical percolation gives the following expressions for the DC conductivity above (Eq. (1)) and below (Eq. (2)) the percolation threshold p_C as a function of the volume concentration of filler [18,21,43]:

$$\sigma_{DC} = \sigma_{0A}\left(\frac{p_A - p_C}{1 - p_C}\right)^t, \quad p > p_C, \quad (2)$$

$$\sigma_{DC} = \sigma_{0M}\left(\frac{p_C - p_A}{p_C}\right)^{-s}, \quad p < p_C, \quad (3)$$

where σ_{0A} and σ_{0M} are the conductivity values of the nanotube agglomerates and polymer matrix, respectively, p_A is the time dependent volume concentration of conducting filler (agglomerates) given by Eq. (1), p_C is the percolation threshold, $t = 2$ and $s = 0.73$ are usually taken for 3D system.

Eqs. (2) and (3), with p_A given by Eq. (1) describe the evolution of the electrical conductivity of a polymer melt with time due to increasing volume concentration of nanotube agglomerates. The classical percolation theory, however, does not describe well insulator–conductor transitions in real two-component systems [21,44,45]. In Eqs. (2) and (3) at the concentration $p_A(t) = p_C$ the conductivity $\sigma_{DC} \to 0$ or ∞, respectively. Experimentally, the conductivity measured over time does not undergo any break down.

A better fit for the dynamic percolation phenomena can be obtained by combining cluster aggregation kinetics (Eq. (1)) with a semi-empirical equation proposed by Fournier et al. [44] and successfully applied to polymers containing CNTs [44–47]:

$$\log \sigma_{DC}(t) = \log \sigma_{0A} + \frac{\log \sigma_{0M} - \log \sigma_{0A}}{1 + \exp(b(p_A(t) - p_C))} \quad (4)$$

where b is the empirical parameter which directs the change in conductance across the percolation threshold. This equation is based on the Fermi-Dirac distribution which describes the non-conductor to conductor transition.

One more equation for the description of the conductivity change in the percolation transition is given by the combined percolation and general effective medium (GEM) theories [48–50]:

$$(1 - p_A(t))\frac{\sigma_{0M}^{1/s} - \sigma_{DC}(t)^{1/s}}{\sigma_{0M}^{1/s} + A\sigma_{DC}(t)^{1/s}} + p_A\frac{\sigma_{0A}^{1/t} - \sigma_{DC}(t)^{1/t}}{\sigma_{0A}^{1/t} + A\sigma_{DC}(t)^{1/t}} = 0 \quad (5)$$

where $A = ((1 - p_C)/p_C)$.

In this section we try to test all three approaches: (1) classical percolation theory for insulator–conductor transition (Eq. (2)), (2)empirical Fournier equation (Eq. (4)), (3)and the general effective

Table 1
Summary of the parameters of fitting.

Composite	σ_{0A}, S/m	$p_{A\infty}$, vol.%	p_{A0}, vol.%	k, s^{-1}	p_C, vol.%	σ_{0m}, S/m	Parameter
Classical percolation							
MWNT/PP, 1.44 wt.%	5×10^{-2}	47	20.85	1.7×10^{-4}	20.8	–	–
MWNT/PP, 2.3 wt.%	5×10^{-2}	61	20.85	2.57×10^{-3}	21	–	–
CB/PP, 5 wt.%	5×10^{-2}	65	20.85	1.7×10^{-3}	21	–	–
Fournier							*b*
MWNT/PP, 1.44 wt.%	0.05912	30	20	0.0012	20	10^{-12}	88.349
MWNT/PP, 2.3 wt.%	0.78715	30	21	0.0012	20	10^{-12}	144.98
CB/PP, 5 wt.%	0.71128	30	20	1.3×10^{-6}	20	10^{-12}	84 100
GEM							*A*
MWNT/PP, 1.44 wt.%	68.92	30	21	0.00042	20	10^{-12}	3.76
MWNT/PP, 2.3 wt.%	75.683	30	21	0.00684	20	10^{-12}	3.76
CB/PP, 5 wt.%	98.43	30	18.3	0.0041	20	10^{-12}	4

medium theory (Eq. (5)) combined with the cluster aggregation model (Eq. (1)) in order to fit the electrical conductivity (1/resistivity) behaviour during melting and annealing of PP composites filled with MWNTs and CB. Figs. 11 and 12 show the results of the fit for the PP/MWNT composites filled with 1.44 wt.% and 2.3 wt.% MWNTs and 5.0 wt.% CB, respectively.

Comparing Figs. 11 and 12 one can see that all three models fit the data with different success. For a very drastic conductivity increase (like in Fig. 11 for 1.44 wt.% MWNTs) good fits are given by both classical percolation and GEM theory. Here, the empirical Fournier model does not work well. However, for the conductivity evolution having part of the curve with linear time dependence (curve for 2.3 wt.% MWNTs in Fig. 11 and for 5.0 wt.% of CB in Fig. 12) the best fit is provided by the empirical Fournier equation. The fit parameters for the three models are given in Table 1. The percolation concentration for the clusters was set to be 20 vol.% close to that for spherical objects [18]. Some further discussion on the physical meaning of the reaction rate k and other parameters can be found elsewhere [18].

4. Conclusion

The effect of melting and re-crystallization of a polypropylene matrix on conductive network formation of MWNTs and CB in CPCs is investigated. The deformation and the re-construction of the conductive networks in MWNT/PP and CB/PP was monitored during non-isothermal and isothermal experiments using inline electrical measurements. Increasing filler content is shown to stabilize the conductive networks preventing them from break down during melting of the composite. MWNTs form a more entangled and stable network compared to CB due to their large aspect ratio. This leads to a time delay in the appearance of the resistivity peak during melting of the MWNTs based CPCs which is not the case for CB filled CPCs.

The aggregation of the MWNTs as well as CB into sphere-like agglomerates is considered to be a main process in the formation of the conductive network in a polymer melt. The network re-construction process during isothermal annealing is explained by re-aggregation of the conductive filler agglomerates. For the modelling of the dynamic network reformation three different approaches are tested: (1) classic percolation theory, (2)general effective medium (GEM)theory and (3)Fournier equation. All three approaches were combined with the cluster aggregation model in order to describe time dependent electrical properties of the composite melts.

Acknowledgement

We would like to thank Nanocyl S.A.(Belgium) for providing the MWNTs in this study. Technical assistance on SEM and TEM study from Dr. Zofia Luklinska and Mr. Mick Willis is also acknowledged.

References

[1] Thostenson ET, Ren Z, Chou TW. Composites Science and Technology 2001;61:1899–912.
[2] Coleman JN, Khan U, Gun'ko YK. Advanced Materials 2006;18:689–706.
[3] Ciselli P, Wang Z, Peijs T. Materials Technology 2007;22:10–21.
[4] Ahir SV, Terentjev EM. Polymer containing carbon nanotubes: active composite materials. In: Nalwa HS, editor. Polymeric nanostructures and their applications. American Scientific Publishers; 2005.
[5] Wang Z, Ciselli P, Peijs T. Nanotechnology 2007;18:455709.
[6] Busfield JJC, Thomas AG, Yamaguchi K. Journal of Polymer Science, Part B: Polymer Physics 2004;42(11):2161–7.
[7] Yamaguchi K, Busfield JJC, Thomas AG. Journal of Polymer Science, Part B: Polymer Physics 2003;41(17):2079–89.
[8] Inam F, Yan HX, Reece MJ, Peijs T. Nanotechnology 2008;19:195710.
[9] Stauffer D, Aharony A. Introduction to percolation theory. Taylor & Francis; 1985.
[10] Zhang R, Baxendale M, Peijs T. Physical Review B: Condensed Matter 2007;76:195431–5.
[11] Celzard A, McRae E, Deleuze C, Dufort M, Furdin G, Mareche JF. Physical Review B: Condensed Matter 1996;53:6209–14.
[12] Munson-McGee SH. Physical Review B: Condensed Matter 1991;43:3331–6.
[13] Bin Y, Mine M, Ai K, Jiang X, Masaru M. Polymer 2006;47:1308–17.
[14] Bryning MB, Islam MF, Kikkawa JM, Yodh AG. Advanced Materials 2005; 17:1186–91.
[15] Sandler JKW, Kirk JE, Kinloch IA, Shaffer MSP, Windle AH. Polymer 2003; 44:5893–9.
[16] Grossiord N, Miltner HE, Loos J, Meuldijk J, Mele BV, Koning CE. Chemistry of Materials 2007;19:3787–92.
[17] Alig I, Lellinger D, Dudkin SM, Potschke P. Polymer 2007;48:1020–9.
[18] Alig I, Skipa T, Engel M, Lellinger D, Pegel S, Potschke P. Physica Status Solidi B-Basic Solid State Physics 2007;244(11):4223–6.
[19] Villmow T, Pegel S, Potschke P, Wagenknecht U. Composites Science and Technology 2008;68:777–89.
[20] Deng H, Zhang R, Bilotti E, Loos J, Peijs T. Journal of Applied Polymer Science 2009;113:742–51.
[21] Alig I, Lellinger D, Engel M, Skipa T, Potschke P. Polymer 2008;49:1902–9.
[22] Alig I, Skipa T, Lellinger D, Potschke P. Polymer 2008;49(16):3524–32.
[23] Deng H, Zhang R, Bilotti E, Peijs T, Loos J. Macromolecular Materials & Engineering, submitted for publication.
[24] Bin Y, Chen QY, Tashiro K, Matsuo M. Physical Review B: Condensed Matter 2008;77:035419.
[25] Bin Y, Kitanaka M, Zhu D, Matsuo M. Macromolecules 2003;36:6213–9.
[26] Zhang R, Dowden A, Deng H, Baxendale M, Peijs T. Composites Science and Technology 2008, doi:10.1016/j.compscitech.2008.11.039.
[27] Wu GZ, Asai S, Zhang C, Miura T, Sumita M. Journal of Applied Physics 2000;88:1480–7.
[28] Zhang C, Ma CA, Wang P, Sumita M. Carbon 2005;43:2544–53.
[29] Zhang C, Wang P, Ma CA, Wu GZ, Sumita M. Polymer 2006;47(1):466–73.
[30] Sumita M, Abe H, Kayaki H, Miyasaka K. Journal of Macromolecular Science-Physics 1986;25:171–84.
[31] Asai S, Sumita M. Journal of Macromolecular Science-Physics 1995;34: 283–94.
[32] Inam F, Peijs T. Adv Compos Lett 2006;15:7.
[33] Nanocyl® 7000 series datasheet. Belgium: Nanocyl S.A.; 2007.
[34] Pantea D, Darmstadt H, Kaliaguine S, Roy C. Applied Surface Science 2003; 217:181–93.
[35] Loos J, Alexeev A, Grossiord N, Koning CE, Regev O. Ultramicroscopy 2005; 104:160–7.
[36] Dondero WE, Gorga RE. Journal of Polymer Science, Part B: Polymer Physics 2005;44:864–78.
[37] Jose MV, Dean D, Tyner J, Price G, Nyairo E. Journal of Applied Polymer Science 2007;103:3844–50.
[38] Xu DH, Wang ZG. Polymer 2008;49:330–8.
[39] Potschke P, Abdel-Goad M, Alig I, Dudkin S, Lellinger D. Polymer 2004;45:8863–70.
[40] Potschke P, Fornes TD, Paul DR. Polymer 2002;43:3247–55.
[41] Lima MD, Andrade MJ, Skakalova V, Bergmann CP, Roth S. Journal of Materials Chemistry 2007;17(46):4846–53.
[42] Heinrich G, Costa FR, Abdel-Goad M, Wagenknecht U, Lauke B, Hartel V, et al. Kautschuk Gummi Kunststoffe 2005;58:163–7.
[43] Kluppel M. The role of disorder in filler reinforcement of elastomers on various length scales. In: Filler-reinforced elastomers scanning force microscopy, vol. 164; 2003. p. 1–86.
[44] Fournier J, Boiteux G, Seytre G, Marichy G. Synthetic Metals 1997;84(1–3): 839–40.
[45] McCullen SD, Stevens DR, Roberts WA, Ojha SS, Clarke LI, Gorga RE. Macromolecules 2007;40(4):997–1003.
[46] Coleman JN, Curran S, Dalton AB, Davey AP, McCarthy B, Blau W, et al. Physical Review B: Condensed Matter 1998;58(12):R7492.
[47] Curran SA, Zhang DH, Wondmagegn WT, Ellis AV, Cech J, Roth S, et al. Journal of Materials Research 2006;21(4):1071–7.
[48] Almond DP, Bowen CR. Physical Review Letters 2004;92(15):157601.
[49] Andrews R., Jacques D., Qian D., Dickey EC. Carbon 2001;39(11):1681–1687.
[50] McLachlan DS, Blaszkiewicz M, Newnham RE. Journal of the American Ceramic Society 1990;73(8):2187–203.